ADVANCED MATERIALS

DOI: 10.1002/adma.200801190

Surface Polarity and Shape-Controlled Synthesis of ZnO Nanostructures on GaN Thin Films Based on Catalyst-Free Metalorganic Vapor Phase Epitaxy**

By *Taeseup Song, Jae Woong Choung, Jea-Gun Park, Won Il Park,* John A. Rogers,** and *Ungyu Paik**

With the rapid developments in nanotechnology, there has been tremendous interest in ZnO-related nanomaterials because ZnO is a wide band-gap semiconductor[1] and a piezoelectric oxide. As a result, it is useful for optoelectronics,[2,3] transparent electronics,[4] sensors,[5] and transducers.[6] ZnO crystals have a noncentral symmetric wurtzite structure and are composed of close packed O^{2-} and Zn^{2+} layers piled alternatively along the c-axis, producing positively charged Zn-terminated (0001) polar surfaces and negatively charged O-terminated $(000\bar{1})$ polar surfaces.[7] Together with the polar surfaces, three fast growth directions of [0001], $[01\bar{1}0]$, and $[2\bar{1}\,\bar{1}0]$ facilitate anisotropic growth of ZnO nanocrystals which have various one-dimensional (1D) structures including c-axis oriented nanowires and a-axis oriented nanobelts.[8,9] For ZnO at the nanometer scale, meanwhile, the surface to volume ratio increases significantly with size reduction and thus, the effect of the surface, especially the surface polarity, plays an important role in determining the structures as well as the chemical and physical properties of the ZnO nanostructures. For example, electrostatic interactions driven by the polar surfaces leads to the deformation of ZnO nanostructures to form unique shapes such as seamless nanorings, nanobows, nanosprings, and nanohelices.[10] In addition, ZnO nanocrystals with varying surface configurations and polarities display different optical and electronic properties. These phenomena make control of the surface is a crucial factor in designing nanomaterials for various applications.[11] Despite the rich family of ZnO nanostructures that can be formed using a variety of methods [10,12–14] synthesis of these nanostructures is very sensitive to the growth conditions and, consequently, often lacking in reproducibility and controllability.

In this paper, we investigate shape-controlled synthesis of vertically aligned ZnO nanostructures on GaN thin films using catalyst-free metalorganic vapor phase epitaxy (MOVPE). MOVPE has several attractive features, including thermodynamic-dependent growth and precise control of partial pressures of the reactants as well as the impurities, which enables the growth of high quality nanomaterials in a controlled manner. The introduction of rough-faceted GaN films leads to selective growth of ZnO nanostructures on the top of hillocks. Decreasing the Zn/O feeding ratios enables ZnO nanostructures ranging from smooth-surfaced nanorod-nanowall networks with non-polar $\{1\bar{1}00\}$ and $\{11\bar{2}0\}$ planes as side faces to corrugated, stacked pyramid-structured nanorods terminated mainly with O-polar $\{10\bar{1}1\}$ and $(000\bar{1})$ planes. More importantly, these ZnO nanostructures exhibit good structural and optical qualities and therefore, provide the opportunity to study surface polarity-dependent luminescent properties by minimizing the effect of surface-related defects.[14]

Micro-faceted GaN films were epitaxially grown on Al_2O_3 (0001) substrates using a vapor transport technique and then transferred to the MOVPE system for growth of ZnO nanostructures. Various types of ZnO nanostructures were obtained by applying different source gas ratios ($DEZn/O_2$) and temperatures. In comparison to ZnO nanorods grown on c-plane Al_2O_3 and/or Si substrates under the same conditions, the degree of vertical alignment of the ZnO nanostructures on the GaN films was significantly improved. This results is consistent with the fact that GaN and ZnO have similar lattice constants with the same wurtzite structure.[15]

Figure 1 shows the morphological evolution of ZnO nanostructures on rough-faceted GaN films as growth conditions vary from Zn-rich and low temperature to O-rich and high temperature. Under relatively Zn-rich and low temperature conditions, vertically-aligned ZnO nanorods networked with nanowalls formed on the entire surface of the GaN layers, as seen in the SEM image of Figure 1a. Upon careful investigation, it is noted that very thin ZnO nanowall networks formed on the rough GaN surface mainly along the chain of

[*] Prof. W. I. Park, Prof. U. Paik, T. Song, J. W. Choung
Division of Materials Science Engineering
Hanyang University
Seoul, 133-791 (Korea)
E-mail: wipark@hanyang.ac.kr; upaik@hanyang.ac.kr
Prof. J. A. Rogers
Department of Materials Science and Engineering
University of Illinois at Urbana-Champaign
Urbana, IL 61801 (USA)
E-mail: jrogers@uiuc.edu
Prof. J.-G. Park
Nano-SOI Process Laboratory, Hanyang University
Seoul, 133-791 (Korea)

[**] This work was supported by the Korea Foundation for International Cooperation of Science & Technology (KICOS) through a grant (K2070400000307A050000310, Global Research Laboratory (GRL) Program) provided by the Korean Ministry of Education, Science & Technology(MEST) in 2008.

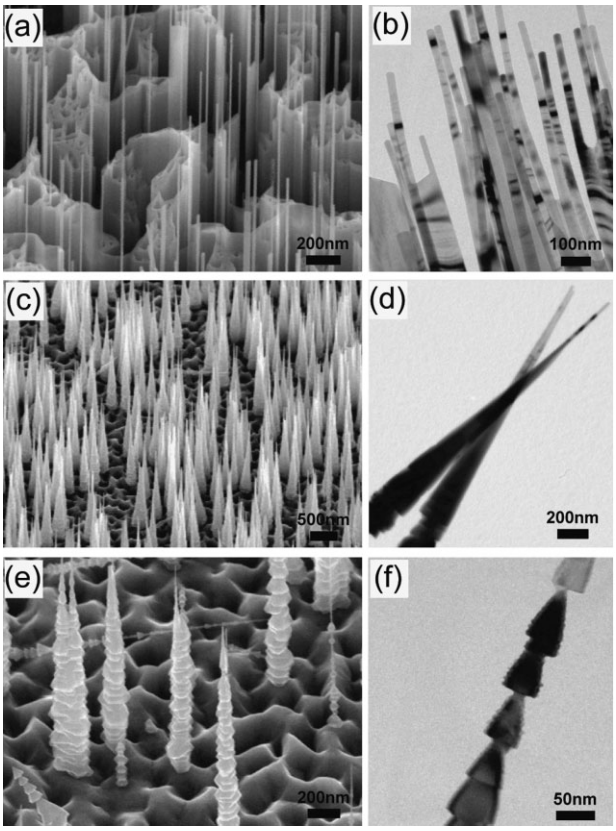

Figure 1. Electron microscopy images of ZnO nanostructures vertically grown on micro-faceted GaN films while varying the growth conditions from Zn-rich and low temperatures to O-rich and high temperatures. a) SEM and b) low magnification TEM images of smooth-surfaced ZnO nanorods networked with nanowalls grown at 700 °C with a $DEZn/O_2$ mole fraction of 1.5×10^{-3}. c) SEM and d) TEM images of corrugated, tapered-structured ZnO nanorods grown at 800 °C with a $DEZn/O_2$ mole fraction of 1×10^{-3}. e) SEM and f) TEM images of corrugated, stacked-pyramid structured ZnO nanorods grown at 800 °C with a $DEZn/O_2$ mole fraction of 5×10^{-4}.

micro-hillocks. ZnO nanorods stand on the nanowalls either at the junction of the nanowalls networks or at the ends of single nanowalls. A low magnification TEM image of the samples shows that the ZnO nanorods have very smooth surfaces and that their diameters are uniform along the length of the rods (Fig. 1b). Both the mean diameter of the nanorods and the thickness of the nanowalls are below 20 nm, which is much smaller than those grown by Au-mediated vapor transport methods.[16]

In contrast, at O-rich and higher temperature conditions, tapered structured, rough-surfaced ZnO nanorods grow out from the tops of micro-hillocks in the GaN film (Fig. 1c). The selective growth of ZnO nanorods on the tops of laterally overgrown GaN micropyramids has been previously reported, where the growth selectivity was attributed to the anisotropic growth habit and absorbate-surface interaction with different surface planes.[17] The low magnification TEM image (Fig. 1d) more clearly shows the morphology of the ZnO nanorods. The diameters of the nanorod tips are almost the same as those of the smooth-surfaced ZnO nanorods grown under Zn-rich and low temperature conditions (~15–20 nm). The diameters of the ZnO nanorods gradually increase and reach ~ 200–400 nm at the bottoms of the nanorods. In addition, corrugated structures with alternatively stacked hexagonal-shaped layers are observed mainly at the bottoms of the nanorods. As the growth conditions shift to more O-rich and high temperature conditions, the corrugated structures spread to the tops of the nanorods (Fig. 1e). The TEM image in Figure 1f reveals that quasi-hexagonal pyramids with average heights and lengths of ~60–70 nm and ~40–50 nm, respectively, stack periodically along the growth direction.

The crystal structures of the ZnO nanostructures were further characterized by high-resolution TEM (HR-TEM). HR-TEM images of nanorods grown under Zn-rich and low temperature conditions reveal highly ordered lattices at both the stem and tip, demonstrating that the nanorods are largely defect-free single crystals (Fig. 2a and b). As shown in Figure 2b, the spacing between adjacent lattice planes stacked along the growth direction is ~0.26 nm, which corresponds to the d-spacing of the (0001) planes, thus confirming that ZnO grow with a c-axis orientation. In addition, no metal particle is observed at the tips, which is a common feature of catalyst-free grown ZnO nanorods. We also characterized the crystal structures of the ZnO nanorod-nanowall junctions. As shown in Figure 2c and d, HR-TEM images show the epitaxial relationship between the nanorods and nanowalls, revealing the monolithically single-crystalline characteristic of the entire structure. In addition, selective area electron diffraction (SAED) patterns taken along the $[11\bar{2}0]$ zone axis (inset of Fig. 2c) together with the measured lattice spacing of the adjacent planes confirm that the vertical and lateral directions of the ZnO nanowalls are [0001] and $[1\bar{1}00]$, respectively.[16] Overall, as shown in the schematic of the ZnO nanorod-nanowall structures in Figure 2d, *c*-axial ZnO nanorods with $\{1\bar{1}00\}$ planes as side faces are connected with nanowalls with $\{11\bar{2}0\}$ side faces and thus, non-polar planes comprise the side faces of the entire nanostructure.

In the case of corrugated ZnO nanorods grown under O-rich and high temperature conditions, the preferential growth direction along [0001] is maintained as confirmed by the SAED pattern as well as by the HR-TEM images (Fig. 3a and b), whereas the side faces are no longer identical to the smooth-surfaced ZnO nanorod $\{11\bar{2}0\}$ planes. Considering the c-axis orientation of the nanorods, the base planes can be identified as O-polar $(000\bar{1})$ planes. In addition, the angle between the main side faces and bases was 62°, which implies that the face is a $\{10\bar{1}1\}$ plane (Fig 3a).[18] Meanwhile, between these two main planes, an approximately 7 nm wide interfacial plane with a face that makes an angle of 118° with the base is clearly identified, indicating that the side face is a $\{10\bar{1}\,\bar{1}\}$ plane (Fig 3a). An enlarged HR-TEM image taken from the black square in Figure 3a shows that the lattice ordering continues to the surfaces with no amorphous layer coated on the surfaces (Fig. 3b). Without considering surface reconstruction, the atomic configuration of the corrugated ZnO nanorods

ADVANCED MATERIALS

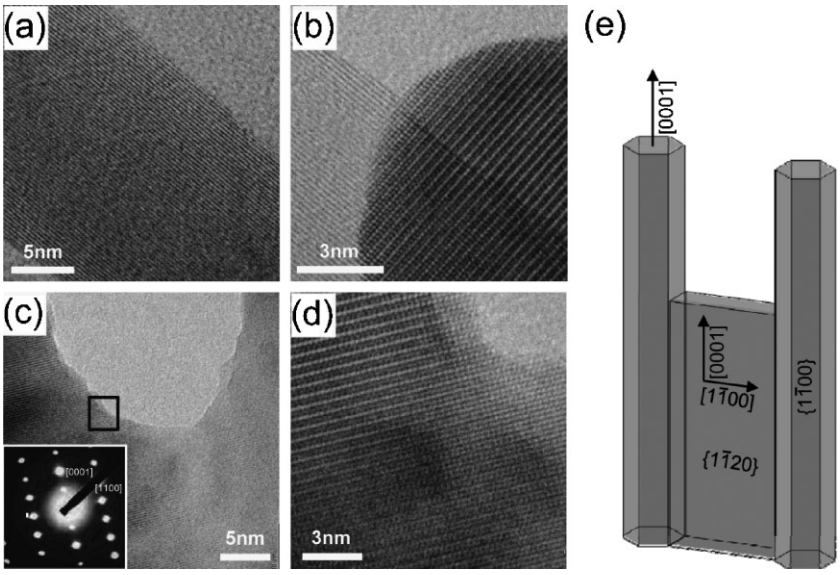

Figure 2. Smooth-surfaced ZnO nanorods networked with nanowalls. a) and b) HR-TEM images of smooth-surfaced ZnO nanorods taken at the nanorod stem and tip, respectively. c) HR-TEM images taken at the junction of the nanorod and nanowall with its corresponding SAED pattern (inset). d)The enlarged HR-TEM image taken from the black square in (c) showing the epitaxial relationship between nanorods and nanowalls. e) The scheme of ZnO nanorods networked with nanowalls.

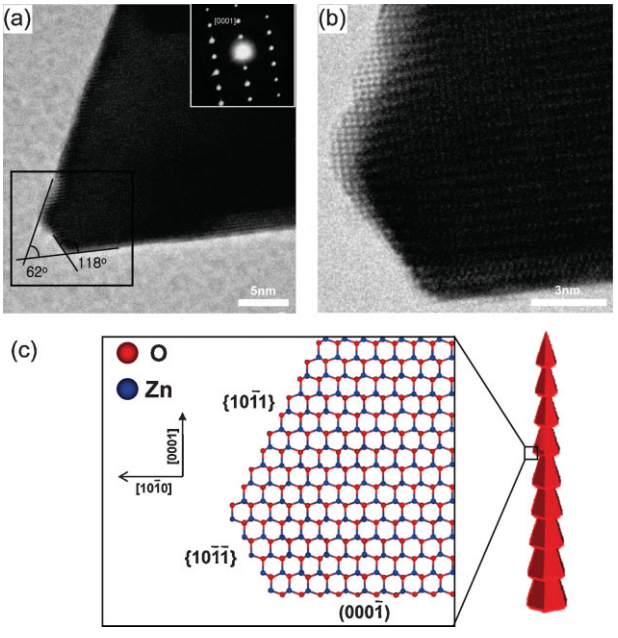

Figure 3. a) HR-TEM images of corrugated ZnO nanorods taken at the edge of a stacked pyramid with its corresponding SAED pattern (inset). b) Enlarged HR-TEM images taken from the black square in (a) showing that the lattice ordering continues to the surfaces. c) Atomic model of stacked-pyramid structured ZnO nanorods projected along [2$\bar{1}\,\bar{1}$0] without surface reconstructions showing that the entire crystals are composed of either O-terminated or Zn-terminated polar surfaces.

projected along the [2$\bar{1}\,\bar{1}$0] direction is described in Figure 3c, which reveals that the entire crystals are composed of either O-terminated or Zn-terminated polar surfaces.[18]

Figure 4 schematically illustrates the growth mechanism of two kinds of smooth-surfaced and stacked-pyramid structured ZnO nanorods on the micro-faceted GaN films. It is well known that the existence of adatoms has a major influence on the surface morphology. They cause the surface to be either smooth or corrugated because adatom diffusion and absorbate-surface interactions are significantly affected by the growth conditions and surface structures.[19–22] To investigate the role of the micro-faceted GaN films in the formation of stacked-pyramid structures, we also grew ZnO nanostructures on bare ZnO buffer layers grown on c-plane Al_2O_3 substrates under the same conditions. In these cases, only smooth-surfaced ZnO nanorods were obtained. Therefore, the formation of ZnO nanorods with corrugated side-surfaces when grown on micro-faceted GaN films is strong evidence that the side facets of the GaN hillocks play important roles in generating the Zn adatoms. Considering that the side facets of GaN hillocks are N-terminated {10$\bar{1}$1},[17] it is proposed that Zn adatoms decomposed from DEZn are easily adsorbed on these surfaces. However, due to the relatively low binding energy between Zn and N, the Zn adatoms can easily desorb or diffuse along the surfaces (Fig. 4a). Meanwhile, the top surfaces of the GaN hillocks, which are Ga-terminated (0001), provide sites for heteroepitaxial growth of c-axis oriented ZnO nanorods because GaN and ZnO have the same crystal structures with a low lattice constant misfit.[17,23] We therefore conclude that c-axis oriented, core ZnO nanorods initially grow on the tops of GaN hillocks and then evolve into stacked pyramid structures due to Zn adatoms produced by the GaN side facets.

The change in morphology from smooth-surfaced to stacked-pyramid structures can be explained by the growth condition-dependent kinetics of surface diffusion and desorption of the adatoms. For the smooth-surfaced ZnO nanostructures (Fig. 4b), low temperature conditions reduce the contribution of the Zn adatoms from the facets of GaN hillocks by either surface diffusion or evaporation. At the same time, Zn-rich conditions result in an excess of Zn layers on the side faces of the ZnO nanorods, consequently reducing the diffusion barrier for the Zn adatoms along ZnO nanorod surfaces. This process allows the production of smooth-surfaced ZnO nanorods and nanowalls.[19,20] Under O-rich conditions at high growth temperatures (Fig. 4c), the number of Zn adatoms that diffuse or desorb from the GaN facets increases while diffusion of the adatoms along the ZnO nanorods is limited by the excess O formed on the ZnO side

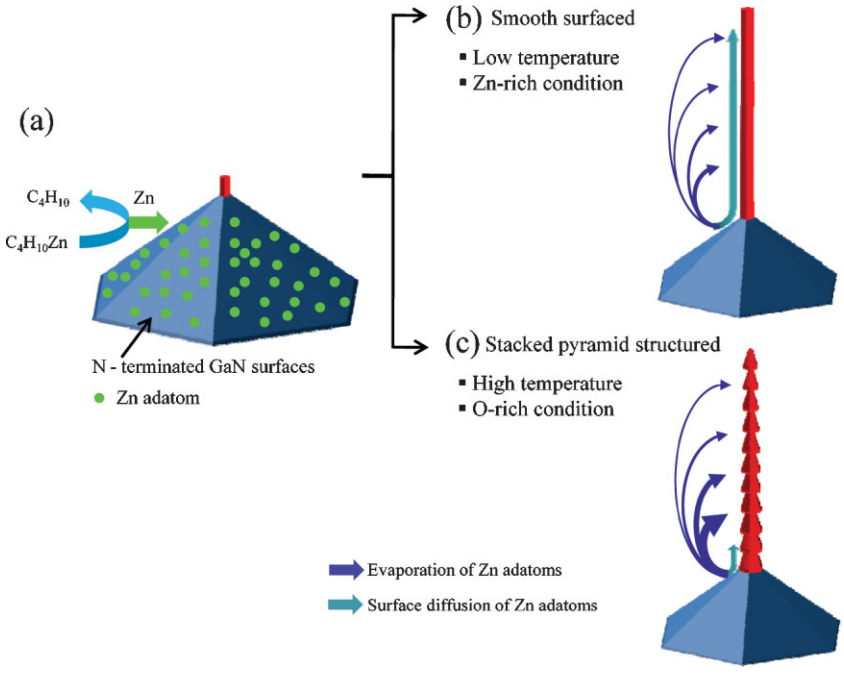

Figure 4. Proposed growth model of stacked pyramid-structured ZnO nanorods vertically grown on micro-faceted GaN films. a) The generation of Zn adatoms on the N-terminated GaN surfaces. The growth mechanisms for b) smooth-surfaced ZnO nanorods and for c) stacked-pyramid structured nanorods.

surfaces, leading to the formation of corrugated ZnO nanorods. Notably, a recent study confirmed that O-terminated surfaces are more chemically inactive than Zn-terminated surfaces[22] and therefore, mainly O-terminated hexagonal pyramid structures as opposed to hexagonal dipyramids (having both O and Zn-terminated) are produced. Only Zn-terminated $\{10\bar{1}\,\bar{1}\}$ planes are observed between O-terminated $(000\bar{1})$ and $\{10\bar{1}1\}$ planes; these may be formed to reduce the total surface energy by minimizing the sharp edges between O-terminated planes.[24]

To investigate the optical properties of the ZnO nanostructures, cathodoluminescence (CL) spectroscopy was employed. At room temperature, ZnO nanorods networked with nanowalls as well as stacked-pyramid structures exhibit strong UV emission peaks at about 3.25 eV with a full widths at a half maximum (FWHM) of ~140 meV (Fig. 5e and f). Compared to the previous CL spectra of ZnO nanowires,[11] these emission peaks can be attributed to the free exciton peaks. Notably, CL images together with the CL spectra taken at the top (T), bottom (B), and whole (W) of each nanostructure show uniform emission from the ZnO nanostructure without any detectable change in position or FWHM of the main CL peaks. More importantly, there is no sign of generation of deep level green emission.[25] Deep level emissions have been observed from various ZnO nanostructures and have been attributed to the surface states and/or defects since the deep level emissions become stronger as either the diameters of nanowires decrease or the surfaces become rougher.[11,25] In contrast to previous reports, the strong free-exciton peaks with very weak deep level emission bands observed in both the smooth-surfaced and corrugated ZnO nanostructures suggest that deep level emission is not directly related to the surface itself but rather, is affected by structural defects easily formed in the surface of nanostructures.

The low temperature (80 K) CL measurements were performed to study the polarity-dependent luminescent properties of the ZnO nanostructures. As shown in Figure 6, the CL spectra of both two kinds of ZnO nanostructures exhibit dominant near-band-edge (NBE) emission peaks with very weak deep level emissions. Considering that both neutral-donor bound exciton and free exciton emission peaks should dominate at 80 K for ZnO,[26] the observed peaks might be attributed to a complex of those emission peaks; it was not possible to observe fine excitonic features due to the peak broadening and limited spectral resolution. Meanwhile, high-resolution CL spectra reveal that the exciton peaks shift from 3.330 eV for smooth-surfaced, non-polar ZnO to 3.345 eV for stack-pyramid, polar ZnO nanostructures. Previous studies on O-polar ZnO epilayers demonstrated that PL peaks shift ~3–5 meV to higher energy due to the residual compressive strain in ZnO layers.[27] However, for the vertically grown 1D nanostructures, the strain induced on the side-surfaces would be very weak and thus, the positions of emission peaks were hardly affected by the strain.[17,28] The shift of ~15 meV is comparable to the energy difference between neutral-donor exciton and free exciton emission peaks.[26,27] We therefore suggest that the CL spectrum of smooth-surfaced ZnO nanostructures is dominated by bound-excitons while the contribution of free-excitons prevails for stacked-pyramid ZnO nanorods terminated mainly with O-polar surfaces. Notably, as indicated by arrow in the inset of Figure 6, an additional peak is observed at ~3.27 eV from stacked-pyramid ZnO nanorods, which is tentatively assigned to longitudinal optical phonon replica since the peak has ~75–80 meV lower energy than the NBE emission, in close agreement with the theoretical calculation by Klingshrin.[29] The increased free-exciton emission together with the presence of phonon replica indicates the high optical quality of the stacked-pyramid ZnO nanorods. Since the O-polar surface is more chemically inert than non-polar or Zn-polar surface, the free-exciton may be less affected by the surface impurity-related band-tail states.[30]

In summary, we demonstrated surface polarity and shape-controlled synthesis of 1D ZnO nanostuctures on the top of micro-faceted GaN hillocks by catalyst free MOVPE. By adjusting the synthesis parameters, smooth-surfaced ZnO

ADVANCED MATERIALS

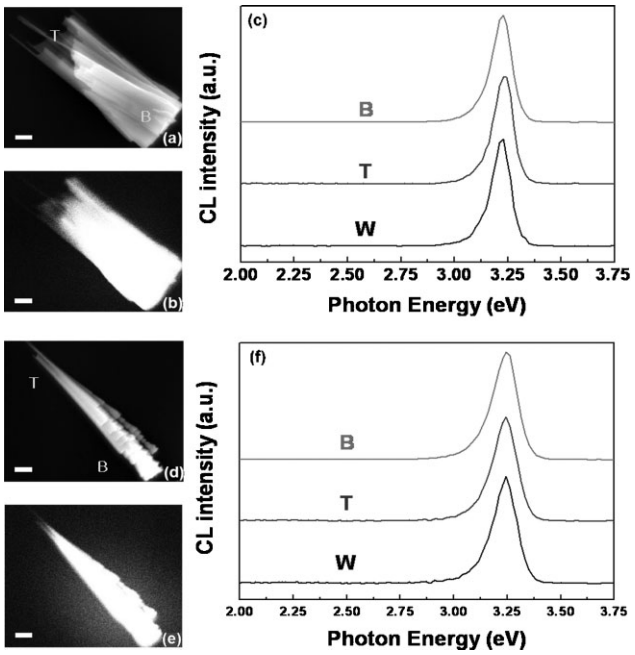

Figure 5. a) FE-SEM and b) room temperature CL images of the nanorod bundles networked with nanowalls and c) their corresponding normalized CL emission spectra. d) FE-SEM image and e) CL image, and f) the corresponding CL spectra of the stacked-pyramid structured ZnO nanorods. The CL spectra were measured in three regions: the whole region, top, and bottom of the two types of nanorods marked by W, T, and B in (c) and (f), respectively. Scale bar: 200 nm.

nanorod-nanowall networks with nonpolar $\{1\bar{1}00\}$ and $\{11\bar{2}0\}$ side surfaces and stacked pyramid-structured ZnO nanorods terminated mainly with O-polar $\{10\bar{1}1\}$ and $(000\bar{1})$ surfaces planes were obtained. We suggest that the morphologies of ZnO nanostructures are dominated by the path of mass transport of Zn adatoms from side facets of GaN hillocks to adjacent ZnO nanorods according to growth conditions. CL measurements reveal strong excitonic emission peaks with extremely low deep level emission for both type of the nanostructures, providing a significant opportunity to understand the surface polarity and shape-dependent luminescent properties of nanoscale materials.

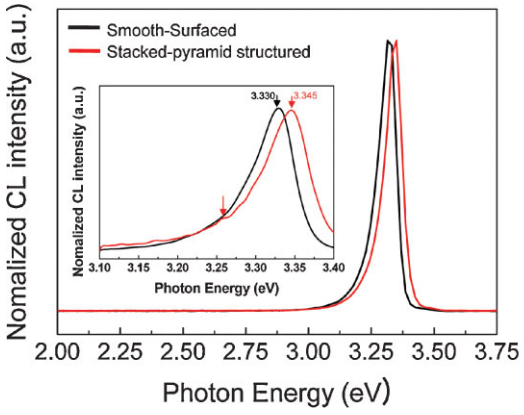

Figure 6. Low temperature CL spectra of the smooth-surfaced and corrugated ZnO nanostructures measured at 80 K. Inset: high-resolution CL spectra.

Experimental

GaN Thin Film Growth: Micro-faceted GaN films were grown on Al_2O_3 (0001) substrates via a vapor transport technique using gallium metal and NH_3 gas as the reactant sources and H_2 as the carrier gas. A Ga source in an alumina crucible was placed in the center of a quartz reactor of a tube furnace. The Al_2O_3 (0001) substrate was located at a distance 3–4 cm downstream from the Ga source. Film growth was carried out at 870 °C using 20 sccm NH_3 and 40 sccm H_2 at 10 Torr for 30 min. As-grown GaN thin films with rough and faceted surfaces were grown epitaxially on Al_2O_3 (0001) substrates with a c-axis orientation as confirmed by x-ray diffraction.

ZnO Nanostructure Growth: The GaN thin films prepared on Al_2O_3 (0001) substrates were transferred to the MOCVD system. For ZnO nanostructure growth, diethylenezinc(DEZn) and oxygen were employed as reactants with argon as the carrier gas. During the growth of ZnO, the growth temperature was controlled in the range of 700–800 °C and the flow rate of DEZn was in the range of 1–3 sccm at a bubbler temperature of −5 °C while the O_2 flow rate was fixed at 20 sccm, producing $DEZn/O_2$ mole fractions of about 5.0×10^{-4}–1.5×10^{-3}.

Characterization of ZnO Nanostructures: The surface morphology and polarity of various types of ZnO nanostructures were characterized using field-emission (FE) SEM (S-4700, Hitachi) and HR-TEM (Jeol-3010). The CL measurements were carried out at room temperature and 80K using a Gatan Mono-CL3 attached to a S-4300SE FE-SEM (Hitachi) with an accelerating voltage of 8 kV.

Received: April 29, 2008
Revised: July 2, 2008
Published online: October 6, 2008

[1] W. Y. Liang, A. D. Yoffe, *Phys. Rev. Lett.* **1968**, *20*, 59.
[2] C. T. white, T. N. Todorov, *Nature* **2001**, *411*, 649.
[3] W. I. Park, G.-C. Yi, *Adv. Mater.* **2004**, *16*, 87.
[4] S. Ju, A. Facchetti, Y. Xuan, J. Liu, F. Ishikawa, P. Ye, C. Zhou, T. J. Marks, D. B. Janes, *Nat. Nanotechnol.* **2007**, *2*, 378.
[5] a) Q. Wan, Q. H. Li, Y. J. Chen, T. H. Wang, X. L. He, J. P. Li, C. L. Lin, *Appl. Phys. Lett.* **2004**, *84*, 3654. b) X. D. Wang, J. Zhou, J. H. Song, J. Liu, N. Xu, Z. L. Wang, *Nano Lett.* **2006**, *6*, 2768.
[6] X. D. Bai, P. X. Gao, Z. L. Wang, E. G. Wang, *Appl. Phys. Lett.* **2002**, *81*, 1869.
[7] C. M. Lieber, *Sci. Am.* **2001**, *285*, 50.
[8] a) A. Wander, F. Schedin, P. Steadman, A. Norris, R. McGrath, T. S. Turner, G. Thornton, N. M. Harrison, *Phys. Rev. Lett.* **2001**, *86*, 3811. b) W. J. Li, E. W. Shi, W. Z. Zhong, Z. W. Yin, *J. Cryst. Growth* **1999**, *203*, 186.
[9] a) H. J. Fan, B. Fuhrmann, R. Scholz, C. Himcinschi, A. Berger, H. Leipner, A. Dadgar, A. Krost, S. Christiansen, U. Gösele, M. Zacjarias, *Nanotechnology* **2006**, *17*, S231. b) Y. Ding, P. X. Gao, Z. L. Wang, *J. Am. Chem. Soc.* **2004**, *126*, 2066.
[10] a) Z. L. Wang, X. Y. Kong, Y. Ding, P. Gao, W. L. Hughes, R. Yang, Y. Zhang, *Adv. Funct. Mater.* **2004**, *14*, 943. b) W. Hughes, Z. L. Wang, *J. Am. Chem. Soc.* **2004**, *126*, 6703. c) X. Y. Kong, Y. Ding, R. S. Yang, Z. L. Wang, *Science* **2004**, *303*, 1348.

[11] a) W.-K. Hong, J. I. Sohn, D.-K. Hwang, S.-S. Kwon, G. Jo, S. Song, S.-M. Kim, H.-J. Ko, S.-J. Park, M. E. Welland, T. Lee, *Nano Lett.* **2008**, *8*, 950. b) A. B. Djurišić, Y. H. Leung, *Small* **2006**, *2*, 944. c) X. Zhou, Q. Kuang, Z.-Y. Jiang, Z.-X. Xie, T. Xu, R.-B. Huang, L.-S. Zheng, *J. Phys. Chem. C.* **2007**, *111*, 12091. d) N. Pan, X. Wang, M. Li, F. Li, J. G. Hou, *J. Phys. Chem. C.* **2007**, *111*, 17265.

[12] a) S. C. Lyu, Y. Zhang, C. J. Lee, H. Ruh, H. J. Lee, *Chem. Mater.* **2003**, *15*, 3294. b) B. D. Yao, Y. F. Chan, N. Wang, *Appl. Phys. Lett.* **2002**, *81*, 757. c) P. X. Gao, Z. L. Wang, *Appl. Phys. Lett.* **2004**, *84*, 2883.

[13] J. B. Mullin, presented at the *Proc. of the Second Int. Conf. on Metalorganic Vapour Phase Epitaxy*, Amsterdam, The Netherlands, April 1984.

[14] X. Zhou, Z.-X. Xie, Z.-Y. Jiang, Q. Kuang, S.-H. Zhang, T. Xu, R.-B. Huang, L. S. Zheng, *Chem. Commun.* **2005**, *44*, 5572.

[15] T. Nakayama, M. Murayama, *J. Cryst. Growth* **2000**, *214/215*, 299.

[16] a) H. T. Ng, J. Li, M. K. Smith, P. Nguyen, A. Cassell, J. Han, M. Meyyappan, *Science* **2003**, *300*, 1249. b) J. Grabowska, A. Meaney, K. K. Nanda, J.-P. Moanier, M. O. Henry, J.-R. Duclère, E. McGlynn, *Phys. Rev. B* **2005**, *71*, 115439. c) J. Y. Lao, J. Y. Huang, D. Z. Wang, Z. F. Ren, D. Steeves, B. Kimball, W. Porter, *Appl. Phys. A* **2004**, *78*, 539.

[17] Y. J. Hong, S. J. An, H. S. Jung, C.-H. Lee, G.-C. Yi, *Adv. Mater.* **2007**, *19*, 4416.

[18] Y. Ding, Z. L. Wang, *Surf. Sci.* **2007**, *601*, 425.

[19] C. Y. Nam, D. Tham, J. E. Fischer, *Appl. Phys. Lett.* **2004**, *85*, 5676.

[20] a) Y. Chen, H.-J. Ko, S.-K. Hong, T. Yao, *Appl. Phys. Lett.* **2002**, *80*, 1358. b) M. Cai, A. B. Djurisic, M. H. Xie, C. S. Chiu, S. Gwo, *Appl. Phys. Lett.* **2005**, *87*, 183103. c) T. Zywietz, J. Neugebauer, M. Scheffler, *Appl. Phys. Lett.* **1998**, *73*, 487.

[21] S. K. Lim, M. J. Tambe, M. M. Brewster, S. Gradecak, *Nano Lett*, in press.

[22] a) P. X. Gao, Z. L. Wang, *Appl. Phys. Lett.* **2004**, *84*, 2883. b) Z. L. Wang, X. Y. Kong, J. M. Zuo, *Phys. Rev. Lett.* **2003**, *91*, 185502.

[23] S. K. Hong, Y. Chen, H. J. Ko, T. Yao, *Acta Phys. Pol. A* **2002**, *102*, 541.

[24] G. Z. Cao, *Nanostructures and Nanomaterials: Synthesis, Properties and Applications*, Imperial College Press, London **2004**, *Ch. 2.*

[25] a) I. Shalish, H. Temkin, V. Narayanamurti, *Phys. Rev. B* **2004**, *69*, 245401. b) A. B. Djurišić, W. C. H. Choy, V. A. L. Roy, Y. H. Leung, C. Y. Kwong, K. W. Cheah, T. K. Gundu Rao, W. K. Chan, H. Fei Lui, C. Surya, *Adv. Funct. Mater.* **2004**, *14*, 856.

[26] W. I. Park, Y. H. Jun, S. W. Jung, Gyu-Chul Yi, *Appl. Phys. Lett.* **2003**, *82*, 964.

[27] a) J. S. Park, J. H. Chang, T. Minegishi, H. J. Lee, S. H. Park, I. H. Im, T. Hanada, S. K. Hong, M. W. Cho, T. Yao, *J. Electron. Mater.* **2007**, *37*, 736. b) O. H. Roh, X. Wang, S. B. Che, Y. Ishitani, A. Yoshikawa, *Phys. Status Solidi C* **2006**, *3*, 1005.

[28] a) Y.-K. Tseng, C.-T. Chia, C.-Y. Tsay, L.-J. Lin, H.-M. Cheng, C.-Y. Kwo, I.-C. Chen, *J. Electrochem. Soc.* **2005**, *152*, G95. b) X. Wang, J. Song, P. Li, J. H. Ryou, R. D. Dupuis, C. J. Summers, Z. L. Wang, *J. Am. Chem. Soc.* **2005**, *127*, 7923.

[29] C. Klingshirn, *Phys. Status Solidi B* **1975**, *71*, 547.

[30] R. E. Sherriff, D. C. Reynolds, D. C. Look, B. Jogai, J. E. Hoelscher, T. C. Collins, G. Cantwell, W. C. Harsch, *J. Appl. Phys.* **2000**, *88*, 3454.